J Mater Sci (2011) 46:3982–3988
DOI 10.1007/s10853-011-5325-y

Anisotropic physical properties of SC-15 epoxy reinforced with magnetic nanofillers under uniform magnetic field

O. Malkina · H. Mahfuz · K. D. Sorge · V. K. Rangari

Received: 20 September 2010 / Accepted: 24 January 2011 / Published online: 5 February 2011

Abstract The mechanical properties of SC-15 epoxy can be significantly enhanced when reinforced with nanofillers. In this study, SC-15 epoxy is loaded with iron oxide nanoparticles and chemically functionalized single-wall carbon nanotubes and cured in a modest magnetic field. Magnetic analysis shows that the iron oxide nanoparticles flocculate to form chains and create a structural anisotropy in the system. Measurements of tensile strength, tensile modulus, and compressive strength in orientations both parallel and perpendicular to the curing field demonstrate an anisotropy in mechanical properties as well, even though there are enhanced properties in all directions. Finally, thermal properties analysis shows that there is a modest shift in the glass transition temperature due to particle inclusion and magnetic flocculation.

Introduction

The SC-15 epoxy is used as a polymer matrix for a number of industrial applications [1, 2]. It has high Young's modulus, excellent adhesion to a variety of substrates, small volume change after curing and low toxicity [3, 4]. In the past, it has been shown that the mechanical properties of polymer epoxies can be greatly improved by the introduction of nanofillers [5–8]. For example, there have been a variety of studies where polymers have been loaded with non-magnetic nanofillers such as TiO_2 [6, 9], SiC [9], carbon nanotubes [10–13], and carbon nanofibers coated with NiO/CoO [14]. These systems were exposed to a uniform high magnetic field during the curing stage [14], inducing structural anisotropy and leading to a clear enhancement of the physical properties of the polymers [6, 10–14].

One drawback of this prior work is the requirement of a very strong magnetic field—sometimes as much as 280 kOe—that requires the use of a liquid helium-cooled superconducting electromagnet. In this investigation, SC-15 epoxy is reinforced with magnetically active nanoparticles and cured in a more modest magnetic field of 10 kOe. Similar enhancement in physical properties is expected even though the applied magnetic field used in this work is significantly lower. Primarily Fe_2O_3 nanoparticles are used as the nanofiller, however, chemically functionalized carbon nanotubes were also added in some cases to prevent any potential microscopic phase separation in the nanocomposites [15]. Even in these much reduced fields, energetics of the system will cause the Fe_2O_3 particles to align in chain-like structures along the field direction. In systems where nanotubes are also involved, the particle alignment can be used to orient the nanotubes. The induced anisotropy in the system that is introduced during the curing process will allow for analysis of the anisotropy in magnetic, structural and mechanical properties in the resultant nanocomposites.

Experimental details

In this work, there are two types of nanofiller-loaded systems that are created and studied. The first system consists

O. Malkina · K. D. Sorge
Department of Physics, Florida Atlantic University, Boca Raton, FL 33431, USA

H. Mahfuz (✉)
Department of Ocean and Mechanical Engineering, Florida Atlantic University, Boca Raton, FL 33431, USA
e-mail: hmahfuz@fau.edu

V. K. Rangari
Center for Advanced Materials (T-CAM), Tuskegee University, Tuskegee, AL 36088, USA

of polymer epoxies mixed with 0.5–2 wt% Fe_2O_3 nanoparticles. These nanoparticles come from a commercially prepared powder with quoted particle diameters of <50 nm. The other system consists of a combination of 1 wt% Fe_2O_3 nanoparticles and 0.2 wt% chemically functionalized single-wall carbon nanotubes (SWCNT(COOH)) in the epoxy. In this case, the commercially prepared nanotubes have a quoted outer diameter of 1–2 nm, a length of 0.5–2 μm and a purity >90% by weight.

The fabrication of these epoxy-based nanocomposites includes four separate stages. First, the nanofillers were ultrasonically mixed for 1 h at room temperature with part A of SC-15 epoxy (60–70% diglycidylether of bisphenol A, 10–20% aliphatic diglyciylether, and 10–20% epoxy toughener). This was done to uniformly distribute the nanoparticles in the low-viscosity fluid and to prevent agglomeration [16]. This mixture was externally cooled during the mixing process to prevent an increase in temperature. Second, a high-speed mechanical stirrer was used to mix the modified epoxy with part B of the epoxy (hardener, consisting of 70–90% cycloaliphatic amine and 10–30% of polyoxyalkylamine). The hardener was added at a volume ratio of 3:10 and the mixture was subsequently vacuum-degassed for 20 min. Next, the mixture was divided and poured into two plastic molds for initial curing. One of the samples was cured at standard room conditions (samples labeled “RCC”) while the other was placed into the most uniform portion of a 10 kOe magnetic field for 6 h (samples labeled “FC”). Previous research has shown [9] that this is sufficient time for the resin to dry completely. Finally, each of these samples is cured for an additional 24 h at standard room conditions, removed from the molds and machined for magnetic and mechanical tests. Measurements on the field cured samples are done both along the curing field (labeled “FC∥”) as well as perpendicular to the curing field (labeled “FC⊥”).

Magnetic measurements on the nanocomposite samples were performed by SQUID magnetometry (Quantum Design MPMS-5) in the temperature range of 5–300 K and applied magnetic fields $|H| < 2$ kOe. For each sample, measured magnetic moments were normalized with respect to the nominal mass of the nanoparticles.

Tensile tests were performed on a Deben Tensile Tester with the load limited to 200 N. We were not able to make a standard test specimen due to small sample sizes. Sandpaper was used at both ends to prevent slipping and breaking of the sample inside of the gripping jaw. Load was applied parallel and perpendicular to the direction of the original curing field and three duplicate test samples of each type were examined. Force and displacement were recorded and converted to stress and strain, respectively.

Compression tests were performed on Zwick/Roell Tester using the standard test method for the compressive properties of rigid plastics [17]. Three duplicate tests on each type of sample were examined. Stress and strain responses were obtained from the force–displacement curve. Force and displacement were recorded and converted to stress and strain, respectively.

Transmission Electron Microscope (TEM) images of the nanocomposite samples were performed using a Jeol-JEM-2010. Samples for TEM were prepared by placing a drop of SC-15/Fe_2O_3 solution on copper grids. One of the grids with SC-15/Fe_2O_3 solution was dried at room condition another one was cured under magnetic field. After complete curing samples on the grids they were analyzed by TEM.

Dynamic Mechanic Analysis (DMA) was performed using a DMA-Q800, operating in the tensile mode at an oscillation frequency of 1 Hz. Experimental data were taken from 25 to 120 °C at a constant scanning rate of 3 °C/min and a soak time of 5 min. While heating, the material was deformed under the tensile force and viscoelastic properties were determined for the deformation.

Thermo-gravimetric analysis (TGA) was conducted with a TA Instruments TGA2950 in nitrogen gas at a heating rate of 10 °C/min. Experimental data were taken from 0 to 800 °C.

Results and discussion

Magnetic analysis

The magnetization curve in Fig. 1 illustrates the effect of field orientation on the sample with 2 wt% Fe_2O_3 nanoparticles. Three orientations are considered—RCC, FC⊥ and FC∥. It is clear from Fig. 1 that the low-field magnetic

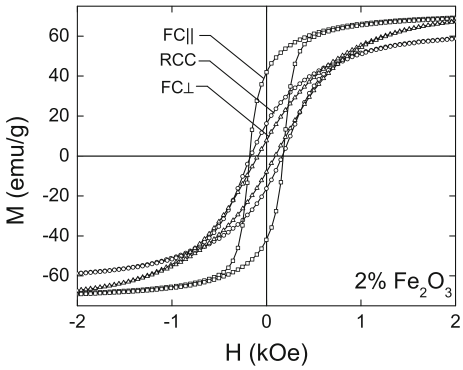

Fig. 1 Magnetization curves at various orientations with respect to the sample curing magnetic field (“FC” samples) in the system with 2 wt% Fe_2O_3 nanofillers. These are put in perspective by the system that had no field curing (“RCC”)

susceptibility for FC|| is much higher than that of the RCC or FC⊥ for all concentrations. This implies that there is an easy magnetic axis as a result of the magnetic anisotropy induced by the curing magnetic field in the case of FC sample. The same results were observed for 0.5 and 1 wt% Fe_2O_3 nanoparticles.

Appearance of an easy axis is due to the flocculation [18] of nanoparticles while in the curing magnetic field [19, 20]. Particles interact in a variety of ways while in the epoxy—repulsive electrical interactions, attractive van der Waals interactions, magnetic dipole–dipole interactions, etc.—but the primary energy of interaction in the presence of the magnetic field is a magnetic dipole–dipole attraction between nanoparticles. While in the curing field, the particles can rotate and agglomerate in chains along the field. The energy of this magnetic attraction [21] between particles is expressed as [22]:

$$U_{Mij} = \sum_{i\neq j}\sum_{j}\frac{\mu_0}{4\pi r_{ij}^3}\left[\left(\vec{\mu}_i\cdot\vec{\mu}_j\right) - 3\left(\vec{\mu}_i\cdot\hat{r}_{ij}\right)\left(\vec{\mu}_j\cdot\hat{r}_{ij}\right)\right] \quad (1)$$

where μ_i and μ_j are the magnetic moments of the particles that are separated by a distance r_{ij}. In this system, the separation between particles is related to concentration of nanofillers in solution.

Another reason to expect this flocculation process during field curing is the reduction of magnetostatic energy when these particles form chains. Long, slender rods with field applied along the axis have a negligible demagnetizing factor with respect to a spherical particle. The magnetostatic energy of an ensemble of particles with a certain magnetization is then reduced when spherical particles align in chains. The driving of this response is only strong when the particles are magnetized. In this system, the particles are magnetized in the curing field, raising the magnetostatic energy. This energy is reduced by the particles forming chains along the curing field lines. This change in ensemble structure is clearly shown by the easy axis exhibited in Fig. 1.

Figure 2 compares the three cases of RCC, FC⊥ and FC|| for a combination of 1 wt% Fe_2O_3 and 0.2 wt% of SWCNT(COOH). There is once again a clear difference between the low-field magnetic susceptibility of FC|| and RCC/FC⊥. The high initial susceptibility of FC|| means that the presence of SWCNT(COOH) does not impede the flocculation of magnetic nanoparticles.

Figure 3 shows magnetization curves that demonstrate the effect of particle concentration on magnetic response. It is clear that there is little difference in initial magnetic susceptibility for all three concentrations (0.5, 1, and 2% Fe_2O_3). One would expect that a system could become too dilute to show anisotropy because of very weak (or even an absence of) interaction between nanofillers. Figure 3 demonstrates that all considered systems are sufficiently concentrated such that interactions influence particle flocculation.

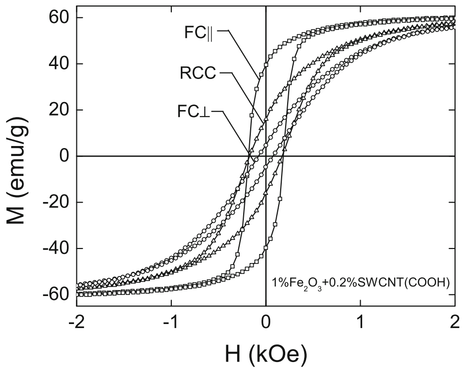

Fig. 2 Magnetization curves at various orientations with respect to the sample curing magnetic field (“FC” samples) in the system with 1%Fe_2O_3 nanofillers and chemically functionalized SWCNTs. The SWCNTs do not impede the flocculation of the magnetic nanoparticles

Mechanical analysis

Typical stress–strain response for the system with 2 wt% of Fe_2O_3 nanoparticles in epoxy are shown in Fig. 4. As in the magnetic analysis, FC samples were studied with load applied parallel and perpendicular to the original curing field. We find that tensile strength is increased in all samples with respect to the neat epoxy. We see a particular enhancement for the case where load is applied along the curing field. This can be explained as a case where the

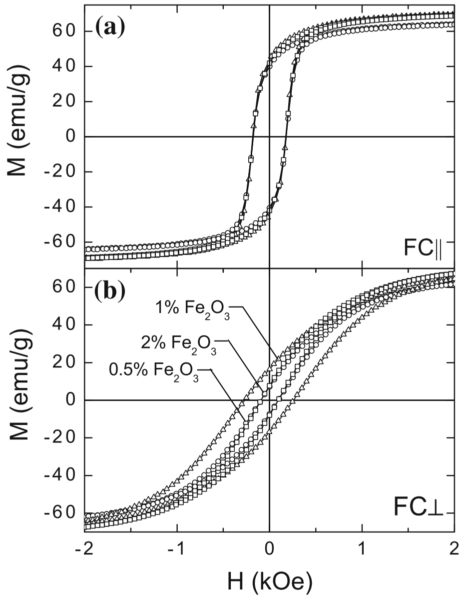

Fig. 3 Magnetization data taken both parallel (**a**) and perpendicular (**b**) to the curing field for samples with varying concentrations of magnetic nanofillers. In each system, there is sufficient particle concentration to show magnetic anisotropy

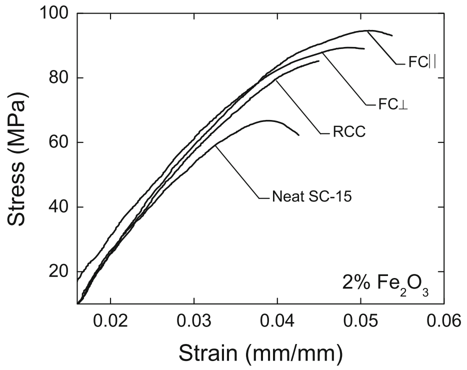

Fig. 4 Tensile stress–strain response of the system with 2 wt% Fe_2O_3 nanofillers. These systems exhibit an enhanced tensile strength and tensile modulus with respect to the neat epoxy, particularly when measured parallel to the sample curing field

nanoparticle chains act as a "backbone" structure that pins the curing epoxy. This backbone is more effective as particle concentration increases to form more substantial chains. While less pronounced, the curves in Fig. 4 also show an enhancement in the tensile modulus. The mechanical properties of these systems are tabulated in Table 1.

If these nanoparticles indeed act as a structure holding the epoxy, chemically functionalized carbon nanotubes should further demonstrate improvement [23]. In this case there would be chemical "anchors" linking the tubes to the structurally pinned epoxy matrix. The stress–strain response for the systems including chemically functionalized nanotubes is shown in Fig. 5. While the tensile strength and tensile modulus are not changed significantly with respect to the systems with particles alone, the modulus of toughness is significantly enhanced. This enhancement is once again most pronounced when load is applied along the curing field direction with toughness of the samples with 1 wt% Fe_2O_3 and 0.2 wt% SWCNT(COOH) (4.8 MJ/m^3) increasing by a factor of 4 over the toughness of neat epoxy (1.3 MJ/m^3). Some degree of alignment may have taken place in the field direction. If particles and nanotubes are aligned, they will share load according to their modulii. This gives FC‖ sample more strength. Since modulus is more or less governed by the rule of mixture at the macroscopic scale, modulus of the nanocomposite is increased. But an interesting phenomenon is observed with the increase in fracture strain with nanotube inclusion. Most likely, grafting of the nanotube surface with COOH groups allow sliding of interfaces between epoxy and nanotubes, causing large tensile deformation. Figure 6 shows a summary of the average experimental results for fracture strain. From this, we see that the fracture strain can be increased by as much as 72% using this nanoparticles chain structuring.

Regular compressive stress–strain response for the system with 2 wt% of Fe_2O_3 in epoxy is shown on Fig. 7. We find an enhancement in compressive strength and modulus in all samples with respect to the neat epoxy. A particular enhancement of 13.7% is detected for the case where load is applied along the curing field with a particle concentration of 2%. All compression test data are collected in Fig. 8.

Transmission electron microscopy

TEM images of RCC and FC samples with 2 wt% Fe_2O_3 concentration are illustrated in Fig. 9. Particles of RCC sample in Fig. 9a are dispersed uniformly and not arranged in any order. To be able to observe the dispersion and arrangement of particles after curing under magnetic field,

Table 1 Tensile properties of neat and reinforced epoxy

Material	Curing time in magnetic field (h)	Tensile strength (MPa)	Gain in strength (%)	Tensile modulus (GPa)	Gain in modulus (%)
Neat Epoxy SC-15	0	60 ± 11.6	–	2.5 ± 0.6	–
0.5% Fe_2O_3	0	72 ± 7.9	20	2.9 ± 0.2	18
0.5% Fe_2O_3(FC‖)	6	85 ± 0.4	43	3.5 ± 0.1	41
0.5% Fe_2O_3 (FC⊥)	6	72.5 ± 0.4	20	3.0 ± 0.1	20
1% Fe_2O_3	0	87 ± 0.9	46	3.3 ± 0.3	33
1% Fe_2O_3(FC‖)	6	93 ± 7.1	55	3.2 ± 0.3	27
1% Fe_2O_3(FC⊥)	6	85 ± 0.7	42	3.1 ± 0.1	24
2% Fe_2O_3	0	90.4 ± 0.6	51	2.79	9
2% Fe_2O_3(FC‖)	6	94.7 ± 0.2	58	3.56	41
2% Fe_2O_3(FC⊥)	6	88.7 ± 1.2	48	2.96	18
1%Fe_2O_3 + 0.2%SWCNT(COOH)	0	85 ± 1.5	42	3.4 ± 0.2	38
1%Fe_2O_3 + 0.2%SWCNT(COOH) (FC‖)	6	95 ± 5.3	59	3.6 ± 0.3	44
1%Fe_2O_3 + 0.2%SWCNT(COOH) (FC⊥)	6	86.9 ± 1.5	45	3.3 ± 0.3	32

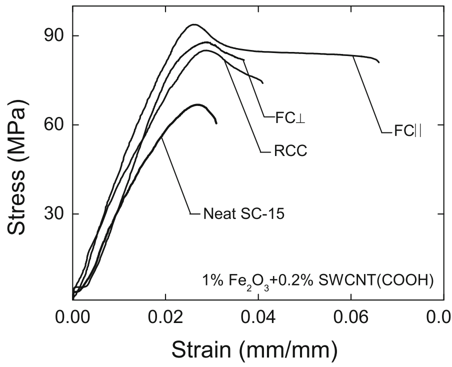

Fig. 5 Tensile stress–strain response of the system with 1 wt% Fe_2O_3 nanofillers and chemically functionalized SWCNTs

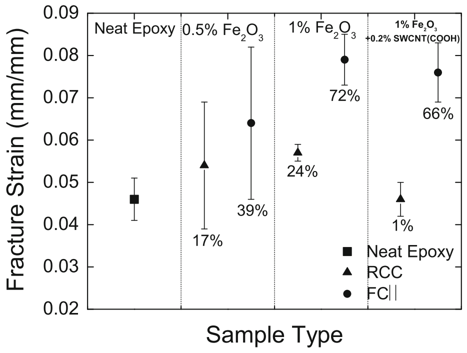

Fig. 6 A plot comparing the fracture strain for various nanofiller concentrations and orientations. Improvement in fracture strain is shown with each symbol

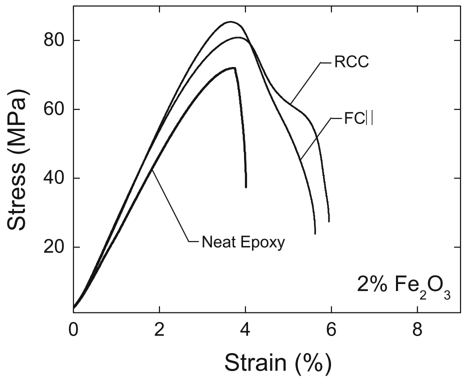

Fig. 7 Compressive stress–strain response of the system with 2 wt% Fe_2O_3 nanofillers

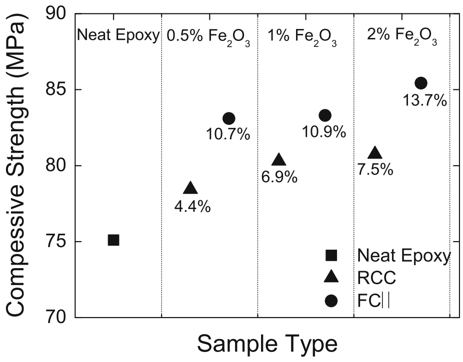

Fig. 8 A plot comparing the compressive strength of various nanofiller concentrations and orientations. Improvement in strength is shown with each symbol

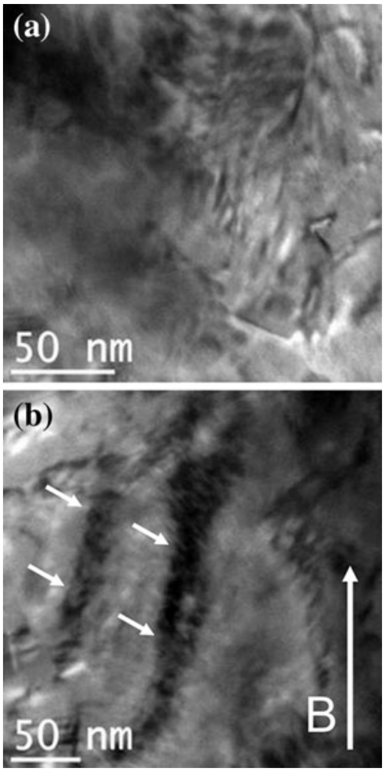

Fig. 9 TEM images of the RCC (**a**) and FC (**b**) nanocomposites of Fe_2O_3 nanoparticles in SC-15 epoxy

TEM was performed to get an image over several microns within the sample as shown in Fig. 9b. These samples were prepared by pouring a droplet of nanoparticle-dispersed resin on to a TEM microgrid through a pipette and then curing them under the magnetic field. The micrograph shows that the Fe_2O_3 nanoparticles are well dispersed, evenly spaced, and aligned along the field direction indicated by the arrow. At least two sets of alignments of particles are indicated by small arrows in Fig. 9b. Thickness of the line is approximately 16 nm. Due to high magnification, it was difficult to see a large number of aligned lines of nanoparticles under TEM. In addition to particles, polymer ligaments are also seen (Fig. 9b) to have aligned along the field direction. Such arrangement of particles and orientation of polymer chains are responsible for enhancement in mechanical and thermal properties of the epoxy indicated earlier.

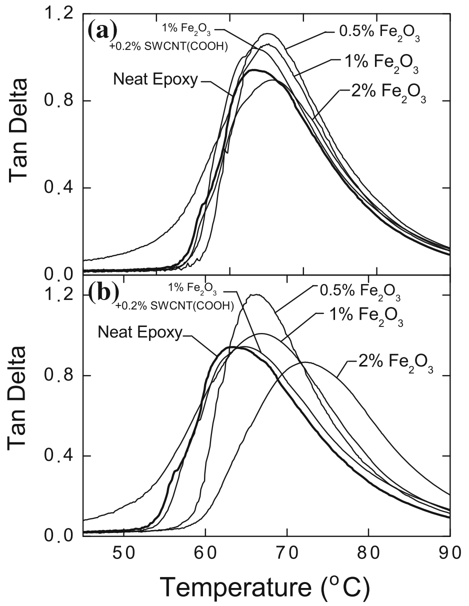

Fig. 10 DMA analysis for (**a**) RCC samples and (**b**) FC∥ samples with respect to neat epoxy

Dynamic mechanical analysis

DMA measurements of the variation of Tan Delta for Fe_2O_3 reinforced epoxies at room conditions are shown in Fig. 10 with respect to neat epoxy. There are no minor peaks at low temperatures. In amorphous polymers like epoxy, the main peak in Tan Delta corresponds to the glass transition temperature T_g of the material. Figure 10a shows that the infusion of Fe_2O_3 alone does not increase T_g to a significant extent. This modest enhancement can be explained by the decreasing free volume of an epoxy (the space in a solid or liquid sample which is not occupied by polymer molecules, i.e., the "empty-space" between molecules) with the addition of nanofillers. DMA results show that iron oxide and SWCNT(COOH)s themselves increase T_g by only 1%. However, by adding nanofillers and curing the sample under a magnetic field, free volume is decreased by additional dipole–dipole interaction between molecules in the polymer. Figure 10b shows that due to this effect Fe_2O_3/epoxy composites cured under a uniform magnetic field have an increase in T_g compared to neat epoxy. Table 2 shows that there is about a 10 °C increase in T_g with 2 wt% Fe_2O_3 nanofillers. This implies that T_g can be increased not only by placing samples in a magnetic field, but also by increasing concentration of Fe_2O_3 nanoparticles in epoxy-based samples cured under a magnetic field.

Thermo-gravimetric analysis

Table 2 T_g of various nanofiller concentrations of FC∥ samples

FC∥ sample	T_g (°C)
Neat Epoxy SC-15	63.3
0.5% Fe_2O_3	66.3
1% Fe_2O_3	67.1
2% Fe_2O_3	72.2
1% Fe_2O_3 + 0.2% SWCNT(COOH)	64.7

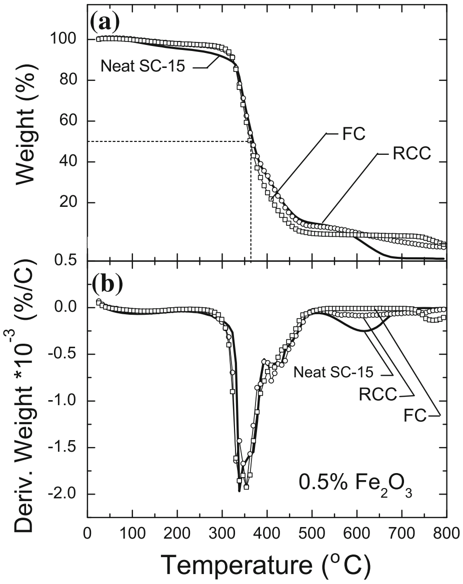

Fig. 11 TGA (**a**) and DTG (**b**) analysis of the 0.5 wt% Fe_2O_3 nanocomposite with respect to that of neat epoxy

Thermo-gravimetric analysis (TGA) was carried out for the neat SC-15 epoxy and Fe_2O_3 RCC and FC nanocomposites to determine the effect of magnetic field on the thermal stability of samples beyond the glass transition temperature. Typical TGA curves for neat SC-15 epoxy and Fe_2O_3 RCC and FC samples are shown in Fig. 11a. As polymers begin to decompose, at a certain temperature weight loss is most dramatic and the derivative curve is steepest at this point. This point is indicated by a peak of the derivative curve (DTG). The peak point in the curve signals is the first stage of decomposition as shown in Fig. 11b. The temperature corresponding to this peak point also coincides with the 50% weight loss point [24–26]. It is observed that all samples start to decompose at around 320 °C and decompose most sharply at 370 °C indicating a rapid decomposition feature. However, there is a difference in the complete decomposition temperatures of these samples: neat SC-15 epoxy decomposes completely at 700 °C, the Fe_2O_3 RCC sample at 760 °C, and the Fe_2O_3 FC sample at 800 °C. A second stage decomposition feature is also observed which is characterized by a small and weak peak in DTG, illustrated in Fig. 11b. For the neat SC-15 epoxy it occurs at 620 °C, for the Fe_2O_3 RCC sample at 640 °C, and for the Fe_2O_3 FC sample at 770 °C. This decomposition is due to extremely slow bleed of about 10–12% weight loss of the epoxy as temperature increases.

Conclusion

In this study, anisotropic mechanical properties of polymer epoxies loaded with nanofillers are investigated. These nanocomposite systems are created by mixing magnetically active Fe_2O_3 nanoparticles and chemically functionalized SWCNTs into nonmagnetic SC-15 epoxy and curing in a magnetic field. A feature of this study is that the use of magnetic nanofillers allows for significant structural anisotropy in the nanocomposites with an application of the modest curing field of 1 kOe.

Magnetic anisotropy in the nanocomposites was detected through DC magnetic measurements. Low-field susceptibility is higher for the case where measurement field is parallel to the curing field, implying a magnetic easy axis in this orientation. This easy axis is the result of the flocculation of magnetic nanoparticles into chains during the curing process. The magnetic anisotropy of the nanocomposites is the signature of a structural anisotropy in the systems.

Anisotropy in mechanical properties was studied through measurements of tensile strength, tensile modulus and compressive strength in orientations parallel and perpendicular to the curing field. In each of the orientations, we see an enhancement in the mechanical properties over those of neat epoxy—implying that nanofillers alone can be advantageous. However, we see particular enhancement for the cases where load is applied parallel to the curing field. In this orientation, we see a 59 and 44% enhancement in tensile strength and tensile modulus, respectively, for the sample with 1 wt% Fe_2O_3 nanofillers and 0.2 wt% chemically functionalized carbon nanotubes. In addition, we see a 13.7% enhancement in compressive strength for the system with 2 wt% Fe_2O_3 nanofillers.

TEM analysis shows the flocculation of Fe_2O_3 nanoparticles along the field direction in FC nanocomposites and the uniform dispersion of nanoparticles in the RCC system.

Changes in thermal properties were detected by performing Dynamic Mechanical Analysis (DMA) in tensile mode. This analysis shows that in RCC samples, there is no shift in the glass transition temperature with nanoparticle inclusion. However, in FC|| samples there is a significant increase in glass transition temperature through higher concentration of Fe_2O_3 nanofillers. This demonstrates that by loading magnetic nanofillers into epoxies, in conjunction with modest magnetic fields, we can substantially enhance mechanical properties of these epoxies without compromising their thermal and viscoelastic properties.

Finally, thermo-gravimetric analysis (TGA) shows that particle inclusion and application of modest magnetic field can substantially change the thermal decomposition behavior of epoxy. Although, the 1st stage decomposition temperatures are identical for all samples, but both the 2nd stage and complete decomposition temperatures increased by more than 100 °C for FC samples.

Acknowledgements The authors would like to acknowledge partial support for this work by the National Science Foundation through Grant # HRD 976871. The authors would also like to thank Dr. Mahmoud Madani at Florida Atlantic University for his assistance in performing mechanical tests.

References

1. Dai L (ed) (2006) Carbon nanotechnology: recent developments in chemistry, physics, material science and device applications. Elsevier Science, Oxford, UK
2. Mahfuz H, Islam M, Rangari VK, Saha M, Jeelani S (2004) Compos B 35:543
3. Banerjee IA, Yu L, Matsui H (2003) Proc Natl Acad Sci USA 100:14678
4. Lazo ND, Grant MA, Condron MC, Rigby AC, Teplow DB (2005) Protein Sci 14:1581
5. Gogotsi Y (2006) Nanomaterials handbook. CRC Press, Boca Raton, FL
6. Xian GJ, Walter R, Haupert F (2006) Compos Sci Technol 66:3199
7. Zhou Y, Farhana P, Rangari VK, Jeelani S (2006) Mater Sci Eng A 426:221
8. Du JH, Bai J, Cheng HM (2007) Exp Polym Lett 1:253
9. Mahfuz H, Zainuddin S, Parker M, Al-Saadi T, Rangari VK, Jeelani S (2007) Mater Lett 61:2535
10. Vasconcelos PV, Lino FJ, Magalhaes A, Neto RJ (2005) J Mater Process Technol 170:277
11. Mahfuz H, Adnan A, Rangari VK, Hasan MH, Jeelani S, Wright WJ, Teresa De (2006) Appl Phys Lett 88:083119
12. Camponeschi E, Vance R, Al-Haik M, Garmestani H, Tannenbaum R (2007) Carbon 45:2037
13. Treacy MMJ, Ebbesen TW, Gibsoj JM (1996) Nature 381:6584
14. Shi D, He P, Lian J, Chaud X, Bud'ko SL, Beaugnon E, Wang LM, Ewing RC, Tournier R (2005) J Appl Phys 97:064312
15. Lin Y, Zhou B, Shiral Fernando KA, Liu P, Allard LF, Sun Y (2003) Macromolecules 36:7199
16. Gojny FH, Wichmann MH, Fiedler B, Schulte K (2005) Compos Sci Technol 65:2300
17. ASTM Standard D695 M (1989) Standard test method for compressive properties of rigid plastics. ASTM International, West Conshohocken, PA
18. Parker MR, van Kleef RPAR, Myron HW, Wyder R (1982) J Magn Magn Mater 27:250
19. Svoboda J (1981) Int J Miner Process 8:377
20. Williams RA, Jia X (1991) Int J Miner Process 33:175
21. De Gennes PG, Pincus PA (1970) Phys Kondens Mater 11:189
22. Rosensweig RE (1985) Ferrohydrodynamics. Cambridge University Press, UK
23. Mahfuz H, Zainuddin S, Parker M, Al-Saadi T, Rangari VK, Jeelani S (2009) J Mater Sci 44:1113. doi:10.1007/s10853-008-3161-5
24. Mahfuz H, Rangari VK, Islam MS, Jeelani S (2004) Compos A 35:453
25. Mahfuz H, Adnan A, Rangari VK, Jeelani S (2005) Int J Nanosci 4(1):55
26. Rodgers RM, Mafhuz H, Rangari VK, Chisholm N, Jeelani S (2005) Macromol Mater Eng 290(5):423